INTEGRATED NUMERICAL SIMULATION OF INJECTION MOLDING USING TRUE 3D APPROACH

Wen-Hsien Yang* Allen Peng, Louis Liu and David C.Hsu
CoreTech System Co.,Ltd., HsinChu, Taiwan, ROC

Rong-Yeu Chang
National Tsing-Hua University, HsinChu, Taiwan 30043, ROC

Abstract

The application of true 3D simulation in the injection molding is becoming popular in the recent years. However, a unified CAE analysis based on solid model for the predictions of molding and warpage of the injection-molded part is seldom reported in the literature due to the numerical and hardware limitations. In this paper, an integrated true 3D approach is developed to simulate the filling, packing and cooling stages in injection molding, as well as the part warpage after ejection. All the simulations can be carried out on the same solid model, in which both cavity and mold base are meshed with solid elements of different topologies. Thanks to the highly efficiency of the proposed methodology, a typical integrated 3D analysis of part with hundred thousand elements can usually be finished on a regular PC within one day. Several numerical examples are reported to indicate the success of the present model

Introduction

The injection molding can be divided into several stages including filling, packing and cooling. Each of these stages can affect the dimension precision and the performance of the molded part after ejection. In the filling stage, the hot polymer melt is injected into the cavity by the applied pressure. After the cavity is completely filled, additional melt is pushed into the cavity at high pressure to compensate the volume shrinkage of the polymer melt during solidification. Usually, once the gated is frozen, the packing phase stops and the cooling phase begin. In the cooling phase, the polymer melt solidifies further until the preset ejected temperature is reached, and then the part is ejected.

CAE (Computer-Aided Engineering) has been widely adopted and proved to be an important tool for part and mold designers. Design and process variables of design are evaluated on computer before the mold is actually constructed. In this manner, potential defects are identified and eliminated in the design phase. In addition to this, design can be refined and even be optimized according to the simulation results, this makes concurrent engineering can be implemented in a cost-efficient way. With the advancement of hardware and theoretical modeling, it's possible now to simulate injection molding process in a more realistic way [1-3].

Conventionally, the 2.5D CAE analysis is used to simulate the injection molding process [4-5]. However, the model simplifications inherent in the 2.5D analysis not only reduces the prediction accuracy but also makes it time consuming to create FEA model. In light of this, true 3D molding simulation becomes increasingly popular in the recent years [6-7]. However, a unified CAE analysis based on solid model for the predictions of molding and warpage of the injection-molded part is seldom reported in the literature due to the numerical and hardware limitations. In this paper, an integrated true 3D approach is developed to simulate the filling, packing and cooling stages in injection molding, as well as the part warpage after ejection. All the simulations can be carried out on the same solid model, in which both cavity and mold base are meshed with solid elements of different topologies.

Governing Equations

Filling Phase:

The polymer melt is assumed to behave as Generalized Newtonian Fluid (GNF). Hence the non-isothermal 3D flow motion can be mathematically described by the followings:

$$\frac{\partial \rho}{\partial t} + \nabla \cdot \rho \mathbf{u} = 0 \tag{1}$$

$$\frac{\partial}{\partial t}(\rho \mathbf{u}) + \nabla \cdot (\rho \mathbf{u}\mathbf{u} - \boldsymbol{\sigma}) = \rho \mathbf{g} \tag{2}$$

$$\boldsymbol{\sigma} = -p\mathbf{I} + \eta(\nabla \mathbf{u} + \nabla \mathbf{u}^T) \tag{3}$$

$$\rho C_P \left(\frac{\partial T}{\partial t} + \mathbf{u} \cdot \nabla T \right) = \nabla(\mathbf{k} \nabla T) + \eta \dot{\gamma}^2 \tag{4}$$

where $\mathbf{u}$ is the velocity vector, T the temperature, t the time, p the pressure, σ the total stress tensor, ρ the density, η the viscosity, k the thermal conductivity, C_p the specific heat and $\dot{\gamma}$ the shear rate. In this work, the

modified-Cross model with Arrhenius temperature dependence is employed to describe the viscosity of polymer melt:

$$\eta(T,\dot{\gamma}) = \frac{\eta_o(T)}{1+\left(\eta_o\dot{\gamma}/\tau^*\right)^{1-n}} \tag{5}$$

with

$$\eta_o(T) = BExp\left(\frac{T_b}{T}\right) \tag{6}$$

where n is the power law index, η_o the zero shear viscosity, τ^* is the parameter that describes the transition region between zero shear rate and the power law region of the viscosity curve. A volume fraction function f is introduced to track the evolution of the melt front. Here, f=0 is defined as the air phase, f=1 as the polymer melt phase, and then the melt front is located within cells with 0<f<1. The advancement of f over time is governed by the following transport equation:

$$\frac{\partial f}{\partial t} + \nabla\cdot(\mathbf{u}f) = 0 \tag{7}$$

The flow rate or injection pressure is prescribed at mold inlet. No slip is assumed at mold wall. Note that only inlet boundary condition is necessary for the hyperbolic transport equation of volume fraction function.

Packing Phase:

In the packing phase the mold cavity is essentially filled up by the polymer melt. More melt are forced by the plunger to fill the cavity in order to compensate the thermal shrinkage after the part is injected and cooled. Therefore, compressible formulation is required for the packing phase. Governing equations are basically the same as listed in (1)-(7). Modified Tait equation is used to model the pvT behavior of the plastic material during the end-of-filling/packing phase.

$$V(P,T) = V(0,T)\left[1 - C\cdot\ln\left(1+\frac{P}{B(T)}\right)\right] + V_t(P,T) \tag{8}$$

where

$$V_o(T) = \begin{cases} b_{1m} + b_{2m}T, T > T_t, \text{melt state} \\ b_{1s} + b_{2s}T, T < T_t, \text{solid state} \end{cases}$$

$$B(T) = \begin{cases} b_{3m}\exp(-b_{4m}T), T > T_t, \text{melt state} \\ b_{3s}\exp(-b_{4s}T), T > T_t, \text{solid state} \end{cases}$$

$$V_t(P,T) = \begin{cases} 0, T > T_t, \text{melt state} \\ b_7\exp(b_8T - b_9P), T > T_t, \text{solid state} \end{cases}$$

$$T \equiv T - b_5$$

$$\textit{transition temperature}: T_t \equiv b_5 + b_6P$$

$$\textit{for amorphous polymers}, b_{1m} = b_{1s}$$

$$\textit{for crstalline polymers}, b_{1m} > b_{1s}$$

Cooling Phase:

During the molding cooling process, a three-dimensional, cyclic, transient heat conduction problem with convective boundary conditions on the cooling channel and mold base surfaces is involved. The overall heat transfer phenomena is governed by a three-dimensional Poisson equation

$$\rho C_P\frac{\partial T}{\partial t} = k\left(\frac{\partial^2T}{\partial x^2} + \frac{\partial^2T}{\partial y^2} + \frac{\partial^2T}{\partial z^2}\right) \quad for \quad \vec{r}\in\Omega \tag{9}$$

where T is the temperature, t is the time, x, y, and z are the Cartesian coordinates, ρ is the density, C_P is the specific heat, k is the thermal conductivity. Equation (9) holds for both mold base and plastic part with modification on thermal properties:

Because mold temperature is fluctuated periodically with time, what we cared is not the actual mold temperature but the effect of the mold temperature on heat transfer of molded part. We can assume there is a cycle-averaged mold temperature that is invariant with time. This cycle-average principle (CAP) is a key concept in the traditional mold-cooling analysis. To reduce the iteration time of the fully transient process, we also introduce the CAP in the calculation of mold temperature. That is, a cycle-averaged temperature distribution of mold base is obtained by solving the following steady-state Laplace equation:

$$k_m\left(\frac{\partial^2\overline{T}}{\partial x^2} + \frac{\partial^2\overline{T}}{\partial y^2} + \frac{\partial^2\overline{T}}{\partial z^2}\right) = 0 \quad for \quad \vec{r}\in\Omega_m \tag{10}$$

where $\overline{T}$ is the cycle-averaged mold temperature.

Warpage Analysis:

After the part is ejected from the mold, a free thermal shrinkage happens due to the temperature difference. Standard three-dimensional solid stress theory can be carried out to simulate the shrinkage and warpage of the molded part as follows.

$$\sigma = \mathbf{C}(\varepsilon - \varepsilon^0 - \alpha\Delta T) \tag{11}$$

$$\varepsilon = \frac{1}{2}(\nabla\mathbf{u} + \nabla\mathbf{u}^T) \tag{12}$$

Where σ is the stress tensor, **C** is a 4th tensor related to the material mechanical properties, ε is the strain tensor, α is CLET tensor and **u** is the displace tensor. Also, the simulated result can exported to commercial general purpose stress solver to run more advanced non-linear stress analysis such as buckling analysis.

Numerical Method

Numerical Discretization Method:

In this paper, a numerical solver based on Finite Volume Method (FVM) is developed to solve the governing equations. The solver has been successfully applied in

injection molding filling simulation [8]. Numerical experiments confirm the reliability and efficiency of the solver.

Integrated Analysis Procedure:

The proposed computation framework is schematically shown in Fig.1. The analysis procedure first reads the input data (including mesh data, material data, and process condition data), performs 3D filling analysis (based on specified uniform mold temperature or mold temperature distribution obtained from previous mold temperature iteration). 3D Cooling analysis is then conducted to obtain part temperature distribution at the end of cooling stage. Cycle-average mold temperature obtained from the cooling analysis fed back to filling modules for improving calculation or serves as an input boundary condition for warpage analysis. The iteration of mold temperature is continued until the mold temperature variation between iterations is small. This integrated analysis ensures a coupling between mold filling and mold cooling results and is of practical value to improve the accuracy of analysis.

Results and Discussion

Fig. 2(a) shows the cavity geometry studied in this paper. It is a two-cavity model with pin gate. The cavity shape is like a semi-sphere shell mounted with a thick rib in the center. The mold base and the coolant layout are shown in Fig. 2(b). Since the injected part geometry is usually quite complicated, it is not easy to mesh the whole model including cavity and mold base by the volumetric elements of the same topology. Therefore, in this paper, we develop a quite flexible numerical method that combination of different element topologies, including hexahedron, prism, tetrahedron and pyramid, are allowed to mesh the model as shown in the Fig. 3(a). Fig.3 (b) is the cut view of the meshed cavity and coolant channel. The cavity is meshed by the tetrahedral element, and the coolant channels are meshed via the combination of prismatic element in the axial direction and the tetrahedral element in the juncture region. The mold base is meshed by the tetrahedral element except in the region adjacent to the coolant surface, where only pyramid element can be used.

Fig. 4(a) is the predicted melt front distribution on the cavity surface. To further demonstrate how the cavity is filled, the iso-surfaces of melt front are plotted in Fig. 4(b). Fig. 5 displays the volumetric shrinkage distributions after packing analysis. The cavity has larger volumetric shrinkage due to the poor pressure transmission through pin gate. Since the core side surface has higher temperature and hence the volumetric shrinkage is also larger over there as shown in Fig. 5(b). The final cavity temperature after several cooling-filling-packing-cooling iterations is shown in Fig. 6. The predicted core side temperature is higher than the other side. This agrees with the experimental observations. In the present numerical model, the mold base is also meshed with volumetric elements, and heat transfer inside the mold base is calculated through the cycle-averaged temperature approach, as a result, we can display the analysis results about the temperature distributions inside the mold base, see Fig 7. Due to the relatively poor heat removal performance of mold base around the secondary runner system, we can see that there is obvious heat accumulation as shown in Fig 7 (c) and (d). Finally, the part deformation predicted from the warpage analysis is shown in Fig 8.

Finally, the analysis performance of the proposed approach for this case is summarized. There are totally 437034 elements in the cavity, 49005 elements in the coolant channel and 588162 elements in the mold base. The maximum memory requirement during calculation is about 572 MB. This case took about 9 hours to complete an integrated analysis on a regular PC with Intel P4 1.7 CPU.

Conclusions

In this paper, an integrated true 3D numerical model for the prediction of injection molding process has been developed. The geometry flexibility and the solution efficiency of the proposed approach have made it a highly reliable CAE tool to aid the designer/engineer to analyze and further optimize the molding process.

Acknowledgement

The authors would like to thank the support from CoreTech Co. and NTHU through the Molding Technology Fundamental Research Project (Project No.0002182).

Reference

[1]. E.C.Bernhardt (Ed.), Computer Aided Engineering for Injection Molding, Hanser (1983)
[2]. T.Manzione (Ed.), Applications of Computer Aided Engineering in Injection Molding, Hanser (1987)
[3]. C.L.Tucker III (Ed.), Fundamentals of Computer Modeling for Polymer Processing, Hanser (1989)
[4]. V.W.Wang, C.A.Hieber, and K.K.Wang, J. Polym. Eng., 7, 21, (1986)
[5]. P.Kennedy, Flow Analysis Reference Manual, Moldflow Pty. Ltd.,Hanser (1993)
[6]. W.B.Young, Polym. Composites, 15, 118 (1994)
[7]. J.F.Hetu, D.M.Gao, A.Garcia-Rejon, and G.Salloum, Polym. Eng. Sci., 38, 223 (1998)
[8]. R.Y.Chang and W.H.Yang, Int. J. Numer. Methods Fluids, 37, 125-148 (2001)

Key Words: Three-Dimensional CAE, Mold Filling,, Integrated Analysis, Injection molding, Numerical Simulation

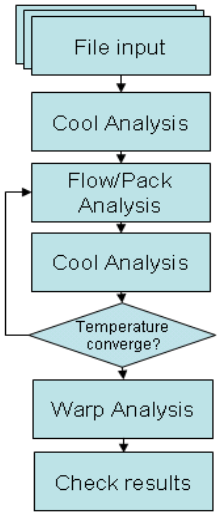

Figure 1.Computational framework of true 3D molding cooling analysis proposed in this work.

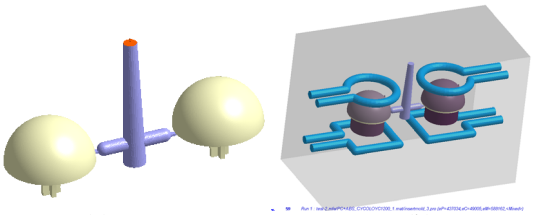

(a) (b)

Figure 2: Configuration of the testing case.

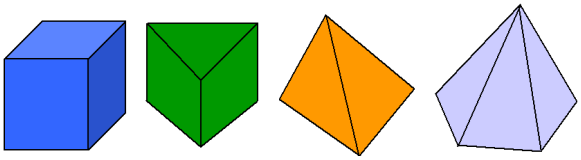

(a)

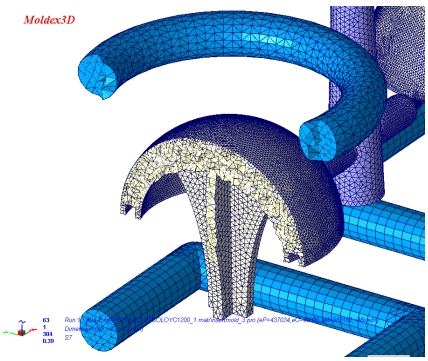

(b)

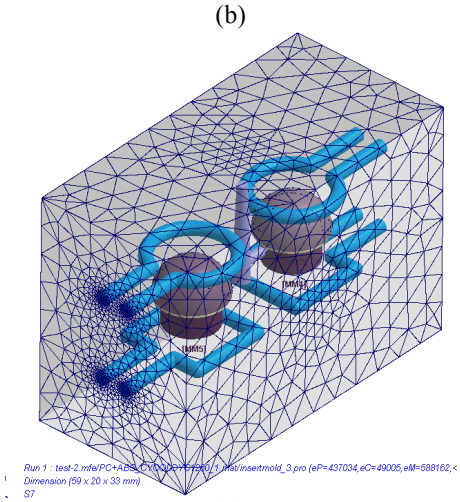

(c)

Figure 3 (a) Supported element shapes in this paper (b) Cut-view of the solid model (c) Surface element of the mold base.

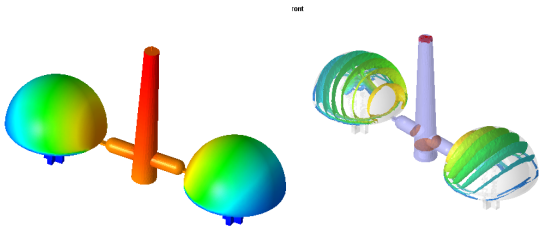

(a) (b)

Figure 4 (a) Predicted melt front distribution on the cavity surface (b) Iso-surface plot of melt fronts.

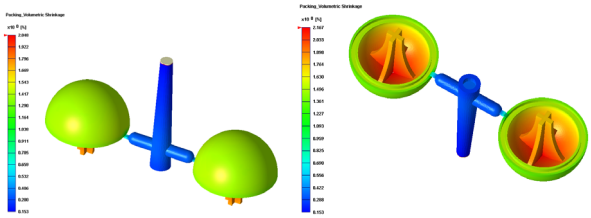

(a) (b)

Figure 5 volumetric shrinkage distributions from packing analysis (a) top view (b) bottom view.

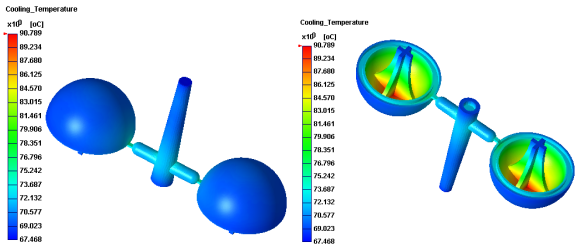

Figure 6 cavity surface temperature distributions from cooling analysis (a) top view (b) bottom view.

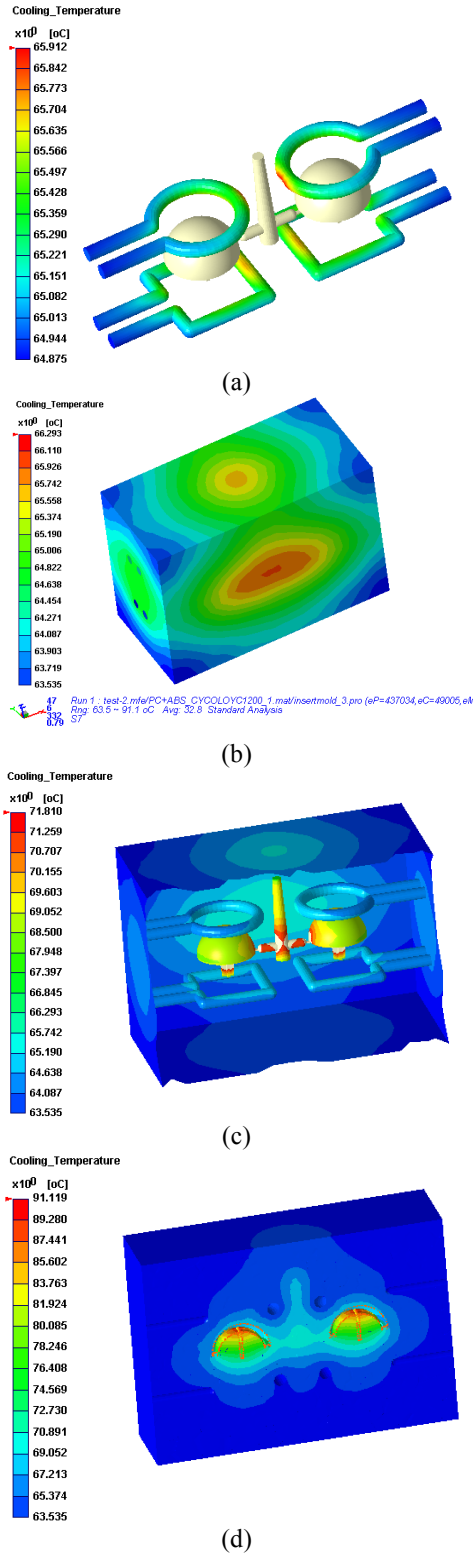

Figure 7 cavity surface temperature distributions from cooling analysis (a) top view (b) bottom view.

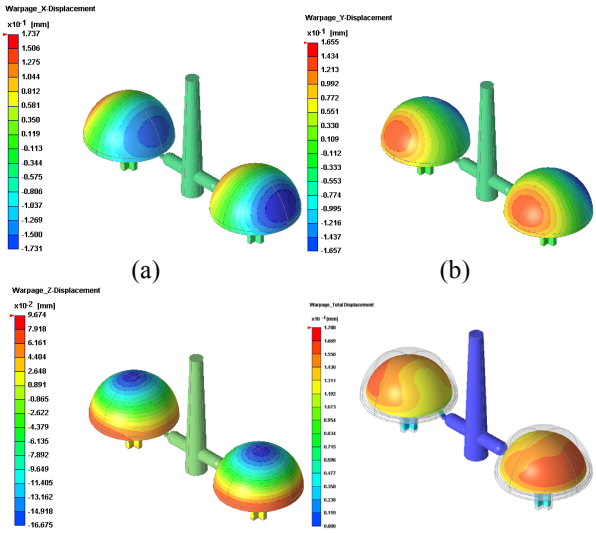

Fig. 8 Warpage analysis result (a) x-displacement (b) y-displacement (c) z-displacement (d) deformation shape